A Trishomocubyl Helical Tubuland Diol Inclusion Host

Roger Bishop,*[a] **Donald C. Craig,**[a] **Ian G. Dance,**[a] **Marcia L. Scudder,**[a]
Alan P. Marchand*[b] **and Yanjun Wang**[b]
[a] *School of Chemistry, The University of New South Wales, Kensington, New South Wales 2033, Australia*
[b] *Department of Chemistry, University of North Texas, Denton, Texas 76203, USA*

All three isomers of 4,7-dimethylpentacyclo$[6.3.0.0^{2,6}.0^{3,10}.0^{5,9}]$undecane-4,7-diol have been prepared and their X-ray structures determined as part of a crystal engineering study into the prediction of new inclusion hosts. The *syn,syn*-isomer **9** forms a double-stranded hydrogen-bonded lattice type [$C_{13}H_{18}O_2$, $P2_1/c$, a 6.3005(5), b 22.372(1), c 7.5313(6) Å, β 96.748(4)°, Z 4, R 0.052] and the *anti,syn* isomer **10** forms a hydrogen-bonded layer lattice [$P2_1/c$, a 12.005(1), b 6.3979(7), c 14.955(1) Å, β 112.767(3)°, Z 4, R 0.045]. In contrast, the *anti,anti*-isomer **11** is a new member of the helical tubuland diol host family [$(C_{13}H_{18}O_2)_3{\cdot}(C_3D_6O)_{1.2}$, $P3_121$, a 12.4957(6), c 7.3076(3), Z 1, R 0.039] containing parallel guest-containing canals with trefoil-shaped cross-section of area 25.4 Å^2.

All of the alicyclic diols **1**–**6** crystallise from ethyl acetate in the same crystal space group $P3_121$ (or its enantiomorph $P3_221$) and each crystal consists of enantiomerically pure material despite commencing from a racemic mixture.[1] The hydrogen bonding network in the solid state results in double helical arrays of diol molecules enclosing series of parallel chiral canals whose topologies and dimensions vary considerably from case to case[2] as shown in Fig. 1. For compounds **3** and **5** these canals are largely filled by part of the diol molecular structure, but the large cross-sectional areas present in crystalline **1**, **2**, **4** and **6** permit these diols to be potent inclusion hosts capable of trapping a wide range of guest species which only interact with the host lattice through van der Waals interactions.[3]

We have termed this family of lattice inclusion materials the helical tubuland inclusion hosts and are interested in the design and synthesis of new members of the family, the investigation of their inclusion properties, and in developing an understanding of the molecular factors which result in this unusual behaviour.[4]

While the above compounds have structural similarities and have the same crystalline form, it is not at all unexpected that other closely related alicyclic diols behave quite differently, since crystal structures cannot normally be predicted,[5] let alone for materials which are combinations of two substances. On the other hand it seems reasonable that there must be underlying structural factors and principles which can be developed into molecular design of new materials.[6]

As part of our earlier work we have attempted to identify the structural features present in the diols **1**–**6** which are essential to their behaving as helical tubulands, and also those redundant structural features which might be modified or even omitted but still allow this lattice to result. These molecular determinants

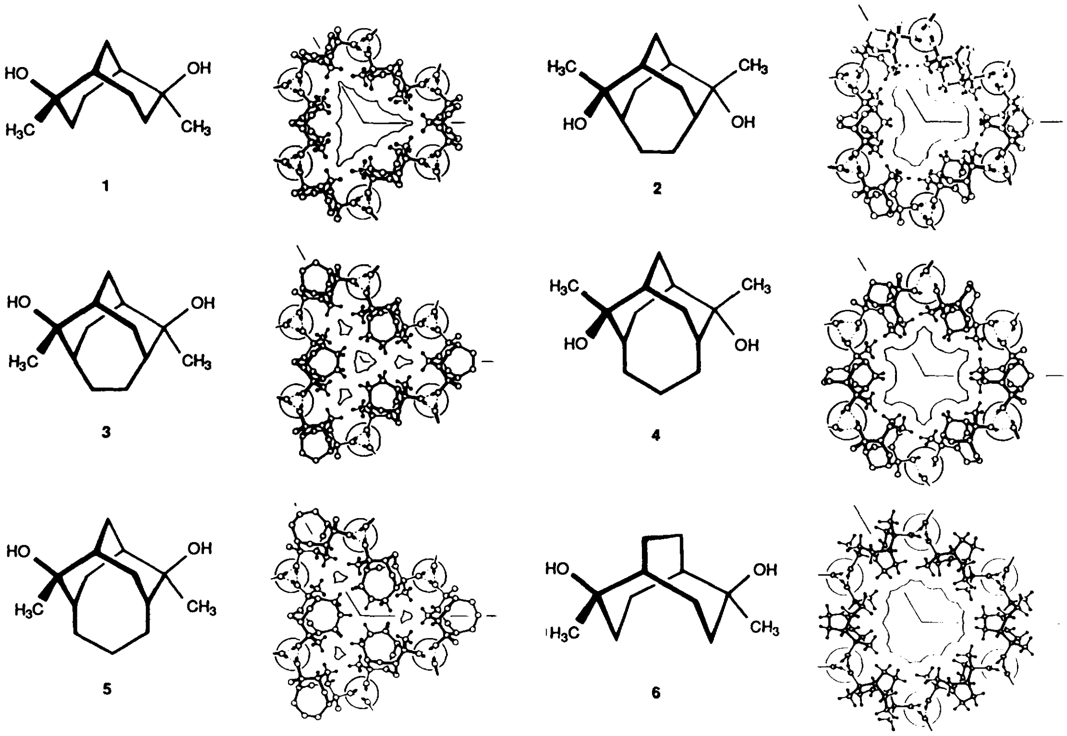

Fig. 1 Projection view in the *ab* plane of one canal only of the helical tubuland lattices of diols **1**–**6**. Key hydrogen atoms defining the van der Waals surface of the host canals are shown as solid black spheres. The hydrogen bonded spines are circled in these diagrams and the hydrogen bonds represented as dashed lines.

define the 'membership rules' of the host family. Based on our previous studies the following tentative molecular determinants were proposed.[7]

(i) The diol molecules must have average C_2 rotational symmetry in solution. However it is not necessary that this be adopted completely in the crystal. For example the diols **4** and **5** cannot adopt exact twofold symmetry in the solid because of the propano bridge.

(ii) The alicyclic structure must be capable of a small degree of flexibility. This allows the skeleton to twist slightly aiding the conformation imposed by the lattice. Thus the rigid adamantane analogue **7** adopts a different crystal structure.

(iii) Substituent groups around the periphery appear so far to be deleterious. Polar groups may disrupt the hydrogen bonding of the host, while substituents in some positions will prevent the diol packing in a helical fashion.

(iv) A bridge on the opposite side to the hydroxy groups is optional. It can therefore be removed or modified in size to control the canal dimensions.

(v) The two hydroxy groups must be separated by a molecular bridge. This performs a key function in buttressing the canal walls against collapse to a denser structure. Thus, for example, the double epimer of **1** adopts a totally different crystal structure involving hydrogen bonded layers.

(vi) The tertiary alcohol groups must have a methyl substituent. This appears to have just the correct size, shape and rigidity to support the canal wall structure. All attempts to replace these groups with others have so far led to different crystal structures being produced.

Results and Discussion

The uncovering of these structural requirements means that it becomes possible to synthesise, by analogy rather than from first principles, new molecules with a predicted crystal structure. Thus new molecules can be targeted which would have a reasonable probability of being new helical tubuland hosts. During such considerations we became interested in whether derivatives of the pentacyclo[6.3.0.0^{2,6}.0^{3,10}.0^{5,9}]undecane (D_3-trishomocubane; *Chemical Abstracts* nomenclature is based on 1,3,5-methenocyclopenta[*c,d*]pentalene) system[8] would show such properties.

The trishomocubanedione **8** was synthesised as described by Smith and Barborak,[9] and bis(methylation) of this compound using methylmagnesium bromide led to a mixture of all three possible diol isomers **9**–**11** (see Scheme 1). These were separated by fractional crystallisation. Diol **10** was clearly identified from its absence of symmetry and the consequent observation of 13 signals in its ^{13}C NMR spectrum. As anticipated, each of the other C_2 symmetric isomers showed a 7 signal spectrum, but it was not obvious which was which at this stage.

The structures of all three diol isomers were obtained by single crystal X-ray determinations. Numerical details of the solution and refinement of these structures are shown in Table 1, and Fig. 2 defines the common crystallographic numbering system adopted. Bond lengths and angles are given in Table 2. Table 3 lists the various dimensions associated with hydrogen bonding in the three crystal structures. In each case the bond lengths and angles obtained for the carbocyclic skeleton are in good agreement with earlier structures carried out on *syn*-4,*syn*-7-diiodopentacyclo[6.3.0.0^{2,6}.0^{3,10}.0^{5,9}]undecane[10] and 1-chloropentacyclo[6.3.0.0^{2,6}.0^{3,10}.0^{5,9}]undecan-7-one-*exo*-11-chlorosulfate.[11]

The first compound isolated and studied was a C_2-symmetric isomer with m.p. 248–249 °C. This proved to be the *syn,syn*-diol **9**. On the basis of our earlier work this compound contravenes the molecular determinant (v) above since it does not have a molecular bridge separating the two hydroxy groups. Therefore our prediction was that **9** would not crystallise with the helical tubuland lattice, and this proved to be correct. Diol **9** crystallised in space group $P2_1/c$ with the molecular structure shown in Fig. 2 and lattice structure in Fig. 3. Four diol molecules each contribute one hydroxy group to produce hydrogen bonded cycles $(\text{–OH})_4$ with, in each case, the second hydroxy group hydrogen bonding to the other hydroxy group of one of the adjacent molecules already involved in the hydrogen bonding network. The network is thus propagated in one dimension only to produce a series of double-stranded columns. Only van der Waals interactions are present between the columns. Alternate columns in the *b* direction are related by the *c* glide. The middle of the $(\text{–OH})_4$ cycle is a centre of symmetry, therefore all diols on the left of the double strand are of the same enantiomer and those on the right of the opposite enantiomer. We have previously encountered a somewhat similar type of hydrogen bonding arrangement in the structure of 2,6-dimethylbicyclo[3.3.1]nona-3,6-diene-*endo*-2,*endo*-6-diol,[12] and suspect that double-stranded columns may be commonplace in C_2 symmetric diols where little steric obstruction exists between the *syn* hydroxy groups.

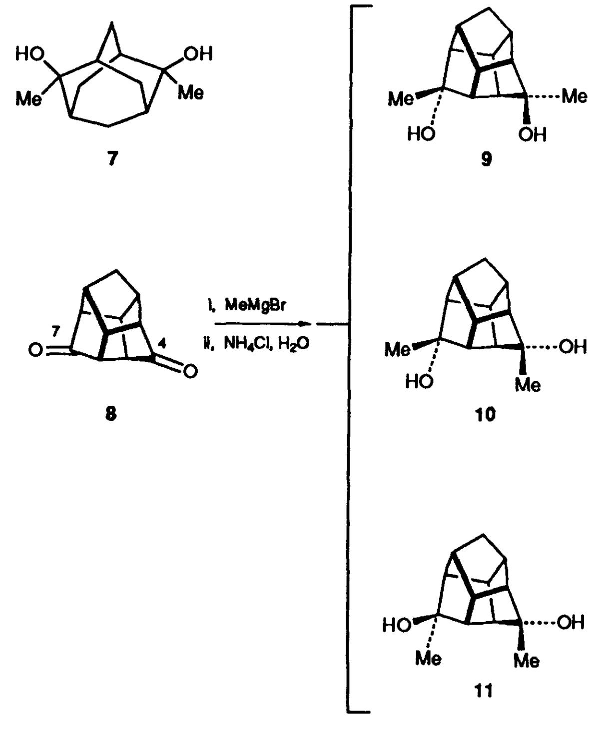

Scheme 1

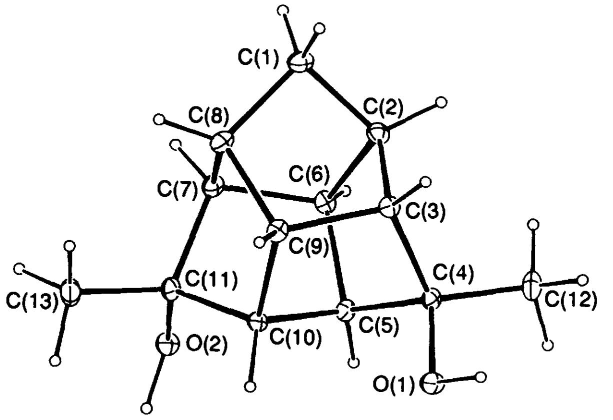

Fig. 2 Molecular structure of **9** showing the common crystallographic numbering system used for the diols **9**–**11**

The *anti,syn*-diol **10** lacks C_2 symmetry and therefore dis-

Table 1 Numerical details of the solution and refinement of structure of diols **9**–**11**

	9	**10**	**11**
Formula, M	$C_{13}H_{18}O_2$, 206.3	$C_{13}H_{18}O_2$, 206.3	$(C_{13}H_{18}O_2)_3{\cdot}(C_3D_6O)_{1.2}$, 695.8
Crystal description	{100}{010}{001}	(010)(−1 − 10)(3 − 20){100}{10 − 2}	Broken fragment
Space group	$P2_1/c$	$P2_1/c$	$P3_121$
a/Å	6.3005(5)	12.005(1)	12.4957(6)
b/Å	22.372(1)	6.3979(7)	12.4957(6)
c/Å	7.5313(6)	14.955(1)	7.3076(3)
β/°	96.748(4)	112.767(3)	90
V/Å^3	1054.2(1)	1059.1(2)	988.14(6)
T/°C	21(1)	21(1)	21(1)
Z	4	4	1
D_{calc}/g cm^{-3}	1.30	1.29	1.17
Radiation, λ/Å	Cu-Kα, 1.5418	Cu-Kα, 1.5418	Cu-Kα, 1.5418
μ/cm^{-1}	6.42	6.39	5.81
Crystal dimensions/mm	0.10 × 0.12 × 0.31	0.09 × 0.40 × 0.11	
Scan mode	$\theta/2\theta$	$\theta/2\theta$	$\theta/2\theta$
$2\theta_{max}$/°	140	140	140
ω scan angle	$(0.80 + 0.15 \tan\theta)$	$(0.50 + 0.15 \tan\theta)$	$(0.60 + 0.15 \tan\theta)$
No. intensity measurements	2251	2286	3740
Criterion for obsd. reflections	$I/\sigma(I) > 3$	$I/\sigma(I) > 3$	$I/\sigma(I) > 3$
No. independent obsd. reflections	1287	1651	1069
No. reflections (m) and variables (n) in final refinement	1287, 136	1651, 136	1069, 90
$R = \Sigma^m\|\Delta F\|/\Sigma^m\|F_o\|$	0.052	0.045	0.039
$R_w = [\Sigma^m w\|\Delta F\|^2/\Sigma^m w\|F_o\|^2]^{\frac{1}{2}}$	0.063	0.064	0.046
$s = [\Sigma^m w\|\Delta F\|^2/(m - n)]^{\frac{1}{2}}$	2.04	2.47	2.49
Crystal decay	None	None	None
Max.. min. transmission coefficients	0.94, 0.83	0.94, 0.84	
R for (no. reflections) measured twice	0.034 (169)	0.011 (71)	0.020 (3043)[a]
Largest peak in final diff. map/e Å^{-3}	0.27	0.18	0.19

[a] Multiple measurements.

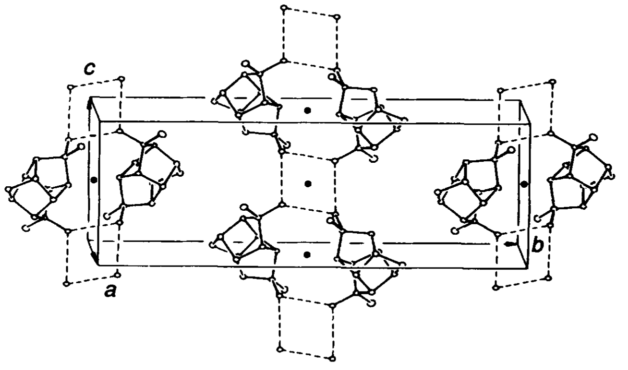

Fig. 3 The unit cell of crystalline **9** showing the arrangement of diol molecules as hydrogen-bonded double-stranded columns. Hydrogen bonds are shown as dashed lines and hydrogen atoms are omitted for clarity.

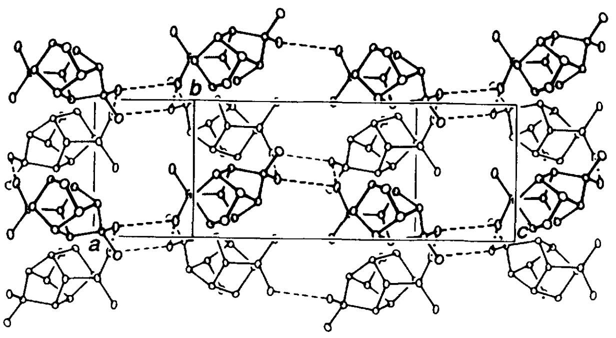

Fig. 4 The crystal structure of **10** showing how the diol molecules are arranged to produce a layer structure constructed using $(\text{-OH})_4$ hydrogen-bonded cycles. Hydrogen bonds are shown as dashed lines and hydrogen atoms are omitted for clarity.

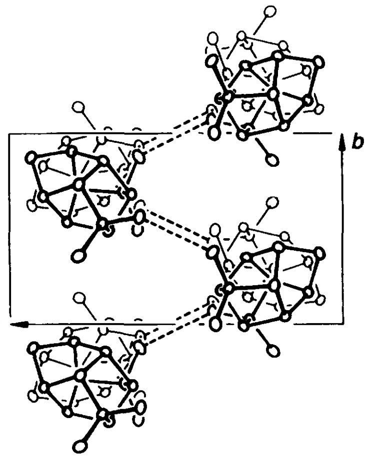

Fig. 5 The unit cell of crystalline **10** viewed along c to reveal the corrugated nature of the hydrogen bonding in the diol layer structure. Hydrogen atoms are omitted for clarity.

obeys molecular determinant (i) and, as expected, this did not have a helical tubuland lattice. It also crystallised in space group $P2_1/c$, but with the more complex hydrogen bonding arrangement illustrated in Fig. 4. Once again four diol molecules each contribute one hydroxy group to produce hydrogen bond cycles $(\text{-OH})_4$, but this time the second hydroxy group is hydrogen bonded to another diol uninvolved in the original hydrogen bonding. The hydrogen bonding network is thus propagated in two dimensions producing a layer structure. We have previously encountered this type of structure amongst a wide range of diol molecules and have found that the layers may be assembled in many different ways based on the $(\text{-OH})_4$ motif.[13] In this instance the hydrogen bonding extends in a corrugated fashion as shown in Fig. 5. Once again, the middle of the $(\text{-OH})_4$ cycle is a centre of symmetry and therefore in this case diol molecules at opposite corners of each cycle are of opposite chirality.

The second C_2 symmetric diol with m.p. 154–156 °C now

Table 2 Bond lengths (Å) and interbond angles (°) for structures **9–11**

	9	**10**	**11**
O(1)–C(4)	1.440(3)	1.435(2)	1.435(2)
O(2)–C(11)	1.451(3)	1.445(2)	
C(1)–C(2)	1.514(4)	1.523(3)	1.522(3)
C(1)–C(8)	1.513(4)	1.524(2)	
C(2)–C(3)	1.529(4)	1.527(2)	1.523(3)
C(2)–C(6)	1.583(4)	1.580(2)	1.567(3)
C(3)–C(4)	1.521(4)	1.520(2)	1.513(3)
C(3)–C(9)	1.561(4)	1.570(2)	1.577(3)
C(4)–C(5)	1.535(3)	1.528(2)	1.520(2)
C(4)–C(12)	1.509(4)	1.518(2)	1.514(3)
C(5)–C(6)	1.572(4)	1.579(2)	1.568(3)
C(5)–C(10)	1.522(4)	1.527(2)	1.525(3)
C(6)–C(7)	1.569(4)	1.572(2)	
C(7)–C(8)	1.537(4)	1.532(2)	
C(7)–C(11)	1.521(4)	1.525(2)	
C(8)–C(9)	1.584(4)	1.572(2)	
C(9)–C(10)	1.575(4)	1.573(2)	
C(10)–C(11)	1.535(3)	1.524(2)	
C(11)–C(13)	1.507(4)	1.512(3)	
C(2)–C(1)–C(8)	95.0(2)	94.5(1)	94.8(3)
C(1)–C(2)–C(3)	103.4(3)	103.2(1)	102.8(2)
C(1)–C(2)–C(6)	105.5(2)	105.5(1)	105.2(2)
C(3)–C(2)–C(6)	97.9(2)	98.5(1)	98.8(1)
C(2)–C(3)–C(4)	103.9(2)	103.7(1)	103.2(2)
C(2)–C(3)–C(9)	99.2(2)	99.0(1)	99.0(2)
C(4)–C(3)–C(9)	105.8(2)	105.2(1)	105.2(2)
C(3)–C(4)–O(1)	112.2(2)	110.5(1)	112.8(2)
O(1)–C(4)–C(5)	108.2(2)	110.9(1)	109.9(1)
O(1)–C(4)–C(12)	109.2(2)	109.1(1)	108.1(1)
C(3)–C(4)–C(5)	93.9(2)	94.5(1)	94.4(1)
C(3)–C(4)–C(12)	116.4(2)	116.1(1)	115.9(1)
C(5)–C(4)–C(12)	116.1(2)	115.1(1)	115.3(2)
C(4)–C(5)–C(6)	105.0(2)	105.1(1)	105.3(1)
C(4)–C(5)–C(10)	103.1(2)	103.3(1)	103.8(1)
C(6)–C(5)–C(10)	98.7(2)	98.6(1)	98.5(1)
C(2)–C(6)–C(5)	104.3(2)	103.9(1)	103.6(1)
C(2)–C(6)–C(7)	103.4(2)	103.4(1)	103.8(2)
C(5)–C(6)–C(7)	104.0(2)	103.7(1)	104.0(1)
C(6)–C(7)–C(8)	98.9(2)	99.2(1)	
C(6)–C(7)–C(11)	105.7(2)	105.0(1)	
C(8)–C(7)–C(11)	103.4(2)	103.8(1)	
C(1)–C(8)–C(9)	105.3(2)	105.4(1)	
C(1)–C(8)–C(7)	103.1(2)	102.9(1)	
C(7)–C(8)–C(9)	98.0(2)	98.4(1)	
C(3)–C(9)–C(8)	103.6(2)	103.7(1)	
C(3)–C(9)–C(10)	103.8(2)	104.0(1)	
C(8)–C(9)–C(10)	104.0(2)	103.9(1)	
C(5)–C(10)–C(9)	98.9(2)	98.7(1)	
C(5)–C(10)–C(11)	103.5(2)	103.0(1)	
C(9)–C(10)–C(11)	105.0(2)	105.9(1)	
O(2)–C(11)–C(7)	109.2(2)	109.8(1)	
O(2)–C(11)–C(10)	111.4(2)	110.8(1)	
O(2)–C(11)–C(13)	109.4(2)	110.0(1)	
C(7)–C(11)–C(10)	94.1(2)	94.1(1)	
C(7)–C(11)–C(13)	116.3(3)	115.6(1)	
C(10)–C(11)–C(13)	115.5(2)	115.6(1)	

must be the *anti,anti*-isomer **11**. This was the compound of greatest interest to us because it satisfies all of the structural requirements outlined above, with the possible exception of (ii). The trishomocubane skeleton is certainly highly rigid which rules out any flexible twisting in any of the three isomers but, because of the geometry of the cage skeleton itself, a degree of prior twisting is already incorporated into the system. It was therefore possible, though by no means certain, that **11** could circumvent the conformational restrictions which we believe prevented the adamantane derivative **7** from forming the helical tubuland lattice.

Crystallisation of **11** from ethyl acetate gave an inclusion compound whose combustion analysis indicated the approximate stoichiometry **11**$_3$·(ethyl acetate). Definite evidence for the presence of ethyl acetate guest molecules was available from the IR and ^{1}H NMR spectra of this material (see Experimental section). These crystals were found to suffer from twinning disorder and were unsuitable for structure determination. The X-ray investigation was therefore carried out on a crystal grown from [^{2}H$_6$]acetone solution. This showed that this isomer crystallised in space group $P3_121$ and did indeed adopt the helical tubuland host lattice (see Fig. 6). The structural necessities of this lattice require the diol molecules in each crystal to be of the same enantiomer, thus the bulk crystalline material is a conglomerate.[14] Refinement of the crystal structure (see Experimental section) confirmed the presence of guest molecules and indicated that six [^{2}H$_6$]acetone molecules were present per five unit cells. This corresponds to the formula **11**$_3$·$(C_3D_6O)_{1.2}$. The canal unobstructed cross-sectional area is trefoil-shaped and rather similar to that of diol **2** but at 25.4 Å^2 is rather smaller than the 30.2 Å^2 of **2**. Fig. 7 shows a typical guest orientation within one canal only of **11**.

Conclusions

The discovery of this new helical tubuland host diol strongly supports our earlier ideas that it is possible to define molecular determinants for multimolecular inclusion hosts, and that these can be used in the deliberate design of new examples of such materials. The cross-ring O–C ··· C–O torsion angles in diols **1** and **4** are 73.8 and 97.4° respectively, but the value for this new helical tubuland diol is markedly different at 163.1° indicating that this parameter is not a significant one in prediction.[7] However, the cross-ring (Me)(HO)C ··· C(OH)(Me) distance in **11** is 3.65 Å which compares closely with the corresponding measurements in **1** and **4** (3.71 and 3.82 Å respectively). Our results show that the helical tubuland diols require a certain amount of twist between the two hydrogen bonding groups to facilitate helicity in the lattice. Previously we had considered a degree of conformational mobility to be essential in allowing this, but these results clearly show that this can also arise through twisting incorporated as part of the alicyclic skeleton. Our previous helical tubuland diols have all involved bicyclic or tricyclic skeletons which incorporated 1,5-bridged cyclooctane systems. The rigid pentacyclic skeleton of **11** is quite dissimilar to these and suggests that a wide range of carbocyclic skeletons will be capable of acting as molecular spacer groups leading to formation of helical tubuland diols hosts provided that the molecular determinants are met.

Experimental

^{1}H (200 MHz) and ^{13}C (50 MHz) NMR spectra were recorded using a Varian Gemini-200 instrument and are reported as chemical shifts (δ) relative to $SiMe_4$. IR spectra were obtained by using a Nicolet 20SXB FTIR spectrometer.

MethylationofPentacyclo[6.3.0.0^{2,6}.0^{3,10}.0^{5,9}]*undecane*-4,7-*dione* **8**.—A stirred solution of **8**^{9} (212.5 mg, 1.22 mmol) in dry diethyl ether (90 cm^3) under nitrogen was cooled externally to *ca.* −10 °C. Methylmagnesium bromide solution in diethyl ether (3 mol dm^{-3}; 13 cm^3; 39 mmol) was added dropwise. After addition was complete, the mixture was stirred at −10 °C for 3 h, and then allowed to warm to room temp. during 3 h. The mixture was quenched by addition of saturated aq. ammonium chloride (50 cm^3), the organic layer separated, and the aqueous phase extracted with diethyl ether (3 × 50 cm^3). The combined ethereal extracts were dried ($MgSO_4$) and solvent evaporated from the filtrate to give a mixture of the three isomeric diols **9**–**11** as a colourless microcrystalline solid (224 mg, 89%). Individual isomers, with data as follows, were obtained *via* fractional recrystallisation. An acetone solution of the mixture

Table 3 Dimensions (Å and °) associated with hydrogen bonding for structures **9**–**11**

9		**10**		**11**	
$O(1)\cdots O(2)^a$	2.775(2)	$O(1)\cdots O(2)^a$	2.749(2)	$O(1)\cdots O(1)^a$	2.809(3)
$HO(1)\cdots O(2)^a$	1.93	$HO(1)\cdots O(2)^b$	1.92	$O(1)\cdots HO(1)^a$	1.86
$O(1)\cdots O(2)^b$	2.796(3)	$H'O(1)\cdots O(2)^a$	1.84		
$O(1)\cdots HO(2)^b$	1.87	$O(1)\cdots O(2)^b$	2.801(2)	$C(4)–O(1)\cdots O(1)^a$	126.46(4)
		$O(1)\cdots HO(2)^a$	1.97	$C(4)–O(1)\cdots O(1)^b$	103.88(4)
$C(4)–O(1)\cdots O(2)^a$	117.35(4)	$O(1)\cdots H'O(2)^b$	1.90	$O(1)^a\cdots O(1)\cdots O(1)^b$	128.91(5)
$C(4)–O(1)\cdots O(2)^b$	140.45(4)			$O(1)–HO(1)\cdots O(1)^b$	168(1)
$O(2)^a\cdots O(1)\cdots O(2)^b$	100.12(8)	$C(4)–O(1)\cdots O(2)^a$	118.30(3)		
$C(11)–O(2)\cdots O(1)^c$	120.77(5)	$C(4)–O(1)\cdots O(2)^b$	143.12(3)	a $1 - y, 1 + x - y, \frac{1}{3} + z$	
$C(11)–O(2)\cdots O(1)^b$	114.06(4)	$O(2)^a\cdots O(1)\cdots O(2)^b$	99.35(5)	b $-x + y, 1 - x, -\frac{1}{3} + z$	
$O(1)^c\cdots O(2)\cdots O(1)^b$	79.88(8)	$C(11)–O(2)\cdots O(1)^c$	136.86(3)		
$O(1)–HO(1)\cdots O(2)^a$	164	$C(11)–O(2)\cdots O(1)^d$	120.50(3)		
$O(2)–HO(2)\cdots O(1)^b$	162	$O(1)^c\cdots O(2)\cdots O(1)^d$	80.65(5)		
		$O(1)–HO(1)\cdots O(2)^b$	161		
a $x, y, 1 + z$		$O(1)–H'O(1)\cdots O(2)^a$	170		
b $1 - x, -y, 1 - z$		$O(2)–HO(2)\cdots O(1)^c$	147		
c $x, y, -1 + z$		$O(2)–H'O(2)\cdots O(1)^d$	172		
		a $1 - x, \frac{1}{2} + y, \frac{1}{2} - z$			
		b $x, \frac{1}{2} - y, \frac{1}{2} + z$			
		c $1 - x, -\frac{1}{2} + y, \frac{1}{2} - z$			
		d $x, \frac{1}{2} - y, -\frac{1}{2} + z$			

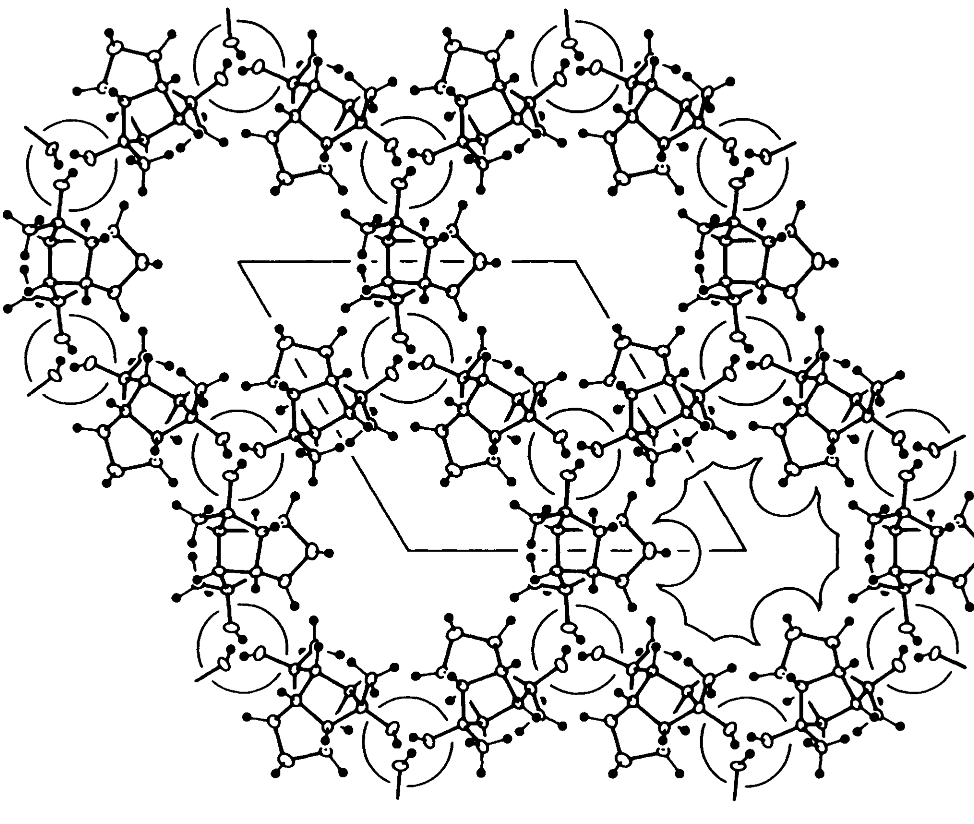

Fig. 6 Projection view in the *ab* plane of the helical tubuland lattice of crystalline **11**. Hydrogen atoms are represented as solid circles and the hydrogen-bonded spines are circled. The unobstructed cross-sectional area of one host canal is shown as a trefoil-shaped area defined by the atomic van der Waals radii.

of isomers was allowed to stand at room temp. After 1 day, diol **9** crystallised out of solution, followed successively by **10** and **11**. The latter compound was initially impure and was further purified by recrystallisation from acetone. A total mass of 208.4 mg (83%) of pure diols was isolated. The remainder of the material was an oil which consisted mainly of **11** by NMR analysis. Analytical samples were obtained by recrystallisation from ethyl acetate.

4,7-Dimethylpentacyclo[6.3.0.0^{2,6}.0^{3,10}.0^{5,9}]*undecane*-syn-4,syn-7-*diol* **9**.*—Yield 35.1 mg (13.9%), m.p. 248–249 °C (Found: C, 75.7; H, 9.0. $C_{13}H_{18}O_2$ requires C, 75.7; H, 8.8%); ν_{max}(paraffin mull)/cm^{-1} 3295w, 2948s, 2930s, 2858s, 1461m and 1377m; δ_H[$(CD_3)_2CO$] 1.26–1.29 (m, 2 H), 1.32 (s, 6 H), 1.62–1.70 (m, 2 H), 2.20–2.40 (complex m, 6 H) and 3.29 (br s, 2 H); δ_C[$(CD_3)_2SO$] 23.7 (q), 33.8 (t), 42.9 (d), 43.2 (d), 54.6 (d), 56.9 (d) and 79.8 (s).

---

* The descriptors *syn* and *anti* are used to indicate relative orientation as defined by the structures shown in the text, and in the same used previously.[10]

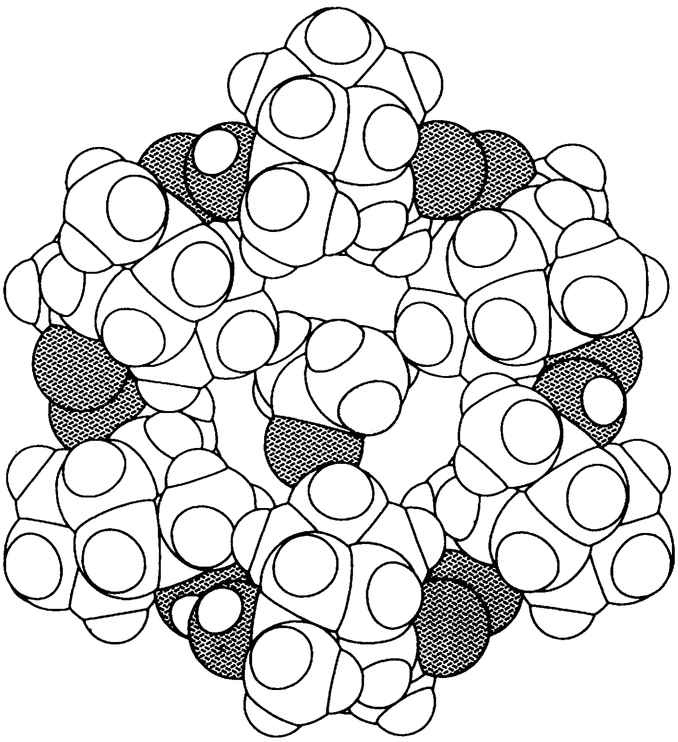

Fig. 7 One canal only of the helical tubulate compound $\mathbf{11}_3\cdot(C_3D_6O)_{1.2}$ viewed along *c* and showing the orientation of a guest molecule within the trefoil-shaped canal. The host diols and [$^2H_6$]acetone are shown in space filling representation.

4,7-Dimethylpentacyclo[$6.3.0.0^{2,6}.0^{3,10}.0^{5,9}$]*undecane*-anti-4,syn-7-*diol* **10**.—Yield 106 mg (42.1%), m.p. 186–187 °C (Found: C, 75.6; H, 8.9. $C_{13}H_{18}O_2$ requires C, 75.7; H, 8.8%); ν_{max}(paraffin mull)/cm^{-1} 3303w, 2943s, 2930s, 2857s, 1459m and 1365m; δ_H[$(CD_3)_2CO$] 1.24 (s, 3 H), 1.26–1.36 (complex m, 3 H), 1.28 (s, 3 H), 1.61–1.72 (complex m, 2 H), 1.75–1.83 (complex m, 1 H), 2.18–2.25 (m, 1 H), 2.25–2.32 (m, 1 H), 2.41 (dq, *J* 5.6 and 1.4 Hz, 1 H), 2.69–2.78 (m, 1 H), 3.34 (br s, 1 H) and 3.40 (br s, 1 H); δ_C[$(CD_3)_2SO$] 23.55 (q), 23.62 (q), 33.3 (t), 41.3 (d), 43.8 (d), 44.4 (d), 44.5 (d), 53.4 (d), 55.2 (d), 56.4 (d), 56.6 (d), 80.2 (s) and 80.3 (s).

4,7-Dimethylpentacyclo[$6.3.0.0^{2,6}.0^{3,10}.0^{5,9}$]*undecane*-anti-4,anti-7-*diol* **11**.—Yield 67.3 mg (26.7%), m.p. 154–156 °C [Found: C, 72.6; H, 9.0. $(C_{13}H_{18}O_2)_3\cdot(C_4H_8O_2)$ requires: C, 73.1; H, 8.8%]; ν_{max}(paraffin mull)/cm^{-1} 3296w, 2940s, 2929s, 2910s, 2858s, 1746w, 1460m and 1376m; δ_H[$(CD_3)_2CO$] diol signals at 1.20–1.35 (complex m, 5 H), 1.23 (s, 3 H), 1.61–1.73 (m, 2 H), 1.73–1.82 (m, 2 H), 2.13–2.25 (complex m, 2 H), 2.68–2.78 (m, 2 H) and 2.84 (br s, 2 H), guest signals at 1.18 (t, *J* 6.0 Hz, 3 H), 1.95 (s, 3 H), 4.04 (q, *J* 6.0 Hz, 2 H) and a water signal at 3.39 (br s); δ_C[$(CD_3)_2CO$] 23.8 (q), 33.7 (t), 44.0 (d), 46.2 (d), 55.1 (d), 57.4 (d) and 81.7 (s).

Crystallography.—Crystals of the three diols were grown from ethyl acetate solution, however those of **11** proved to be twinned and so the sample eventually used was obtained by slow evaporation of a $(CD_3)_2CO$ solution.

Reflection data for crystals of **9–11** were measured with an Enraf–Nonius CAD-4 diffractometer in $\theta/2\theta$ scan mode using nickel-filtered copper radiation (λ 1.541 78 Å). Data were corrected for absorption, except for **11** since the material used was a broken fragment. Reflections with $I > 3\sigma(I)$ were considered observed. The positions of all non-hydrogen atoms of the diol were determined by direct phasing (MULTAN 80).[15] Hydroxy hydrogen atoms were located in a difference Fourier map. In the case of **10**, each was disordered and both components were included in the refinement with occupancy 0.5. For all three structures all other hydrogen atoms were included in calculated positions; all hydrogen atoms were assigned thermal parameters equal to those of the atom to which they were bonded. Positional and anisotropic thermal parameters for the non-hydrogen atoms were refined using full matrix least sqares (BLOCKLS, a local version of ORFLS).[16] Reflection weights used were $1/\sigma^2(F_o)$, with $\sigma(F_o)$ being derived from $\sigma(I_o) = [\sigma^2(I_o) + (0.04I_o)^2]^{\frac{1}{2}}$. Atomic scattering factors and anomalous dispersion parameters were from International Tables for X-ray Crystallography.[17]

For **11** it was clear at this stage that there was still some residual electron density which had not been incorporated in the model for the structure. Since the diol molecules had adopted the helical tubuland structure it was not surprising that the diol was part of a host–guest system. Since the crystals had been grown from $(CD_3)_2CO$ this was expected to be the guest. The difference map showed two peaks approximately 1.5 Å apart which were adjacent to other pairs to form an infinite spiral of peaks. Three of these peaks were selected, and were overlaid against the three C atoms of a model of acetone. There were two possible selections here, with each of the original two peaks on the difference map being positioned at the central C atom of the acetone molecule. Preliminary refinement of both options was carried out using RAELS, a least squares program allowing rigid body refinement.[18] One option gave a significantly lower *R* factor, so refinement was completed from this model. The acetone molecule was refined as a rigid group with a 12 parameter ***TL*** thermal group (where ***T*** is the translation vector and ***L*** is the libration vector). The occupancy of the acetone was refined and converged to 0.22. Refinement was completed with this set to 0.20, a value which corresponds to six acetone molecules per five unit cells of the canal. The final residual *R* = 0.039 and the largest peak in the final difference map was 0.19 e Å^{-3}. Calculated densities for the guest-free host lattice and the inclusion compound were 1.05 and 1.17 g cm^{-3} respectively. The experimentally observed density, obtained by flotation in CCl_4–cyclohexane, was 1.17 g cm^{-3}.

ORTEP-II[19] running on a Macintosh IIcx was used for the structural diagrams, and an IBM 3090 computer was used for all calculations. Chem 3D was also used to generate diagrams of **11**. Supplementary structural data consisting of thermal and positional parameters and torsional angles, have been deposited at the Cambridge Crystallographic Data Centre (CCDC). For details, see 'Instructions for Authors 1993,' *J. Chem. Soc., Perkin Trans. 2*, 1993, issue 1.

Acknowledgements

This work has been supported by the Australian Research Council. A. P. M. thanks the Robert A. Welch Foundation (Grant B-963) and the Office of Naval Research (Contract N00014-92-J-1362) for financial support of this study.

References

1 I. G. Dance, R. Bishop, S. C. Hawkins, T. Lipari, M. L. Scudder and D. C. Craig, *J. Chem. Soc., Perkin Trans. 2*, 1986, 1299; R. Bishop, D. C. Craig, I. G. Dance, S. Kim, M. A. I. Mallick, K. C. Pich and M. L. Scudder, *Supramolecular Chem.*, in the press.

2 I. G. Dance, R. Bishop and M. L. Scudder, *J. Chem. Soc., Perkin Trans. 2*, 1986, 1309.

3 R. Bishop and I. G. Dance, in *Inclusion Compounds*, eds. J. L. Atwood, J. E. D. Davies and D. D. MacNicol, Oxford University Press, Oxford, vol. 4, 1991, pp. 1–26; R. Bishop and I. G. Dance, *Top. Curr. Chem.*, 1988, **149**, 137.

4 A. T. Ung, R. Bishop, D. C. Craig, I. G. Dance and M. L. Scudder, *Struct. Chem.*, 1992, **3**, 59; A. T. Ung, R. Bishop, D. C. Craig, I. G.

Dance and M. L. Scudder, *J. Chem. Soc., Perkin Trans. 2*, 1992, 861.

5 A. Gavezzotti, *J. Am. Chem. Soc.*, 1991, **113**, 6622; J. Maddox, *Nature (London)*, 1988, **335**, 201.

6 G. R. Desiraju, *Crystal Engineering: The Design of Organic Solids*, Elsevier, Amsterdam, 1989.

7 R. Bishop, I. G. Dance, S. C. Hawkins and M. L. Scudder, *J. Incl. Phenom.*, 1987, **5**, 229.

8 A. P. Marchand, *Chem. Rev.*, 1989, **89**, 1011.

9 E. C. Smith and J. C. Barborak, *J. Org. Chem.*, 1976, **41**, 1433.

10 A. P. Marchand, T.-C. Chou, J. D. Ekstrand and D. van der Helm, *J. Org. Chem.*, 1976, **41**, 1438.

11 G. A. Tolstikov, B. M. Lerman, F. Z. Galin, Yu. T. Struchkov and V. G. Andrianov, *Tetrahedron Lett.*, 1978, 4145.

12 M. A. I. Mallick, R. Bishop, D. C. Craig, I. G. Dance and M. L. Scudder, *Aust. J. Chem.*, 1991, **44**, 343.

13 S. C. Hawkins, M. L. Scudder, D. C. Craig, A. D. Rae, R. B. Abdul Raof, R. Bishop and I. G. Dance, *J. Chem. Soc., Perkin Trans. 2*, 1990, 855.

14 J. Jacques, A. Collet and S. H. Wilen, *Enantiomers, Racemates and Resolutions*, Wiley, New York, 1981, ch. 2.2.

15 P. Main, MULTAN 80, University of York, England, 1980.

16 W. R. Busing, K. O. Martin and H. A. Levy, ORFLS, Oak Ridge National Laboratory, Tennessee, USA, 1962.

17 J. A. Ibers and W. C. Hamilton, eds., *International Tables for X-Ray Crystallography*, vol. 4, Kynoch Press, Birmingham, 1974.

18 A. D. Rae, *RAELS, A comprehensive constrained least squares refinement program*, University of New South Wales, 1989.

19 C. K. Johnson, ORTEP-II, Oak Ridge National Laboratory, Tennessee, USA, 1976.

Paper 3/00070B
Received 5*th January* 1993
Accepted 1*st February* 1993